Incorporation of the Detector Resolution Compensation (DRC) in the Ordered-Subset Transmission (OSTR) Algorithm for Transmission Imaging in SPECT

Bing Feng, Jeffrey A. Fessler, and Michael A. King

Abstract— **In order to reconstruct attenuation maps with enhanced resolution and accuracy, we developed a method of incorporating the detector resolution compensation (DRC) in the ordered-subset transmission (OSTR) algorithm for transmission imaging, which approximately models the blur caused by the finite intrinsic detector resolution, the non-ideal source collimation and detector collimation. We derived the formulation using the optimization transfer principle as in the derivation of the OSTR algorithm. The formulation includes one forward-blur step and one back-blur step, which do not severely slow down reconstruction. The formulation could be applicable to various transmission geometries, and easily adapted to compensation for finite energy resolution of the transmission system. We used a digital rod phantom to validate our method.**

I. INTRODUCTION

IN SPECT attenuation and finite distance-dependent resolution of the detector are two sources of image degradation [1-4]. Patient-specific attenuation map is needed to perform accurate attenuation compensation (AC). Attenuation maps are normally obtained from transmission acquisition using various transmission sources (Ba-133, Tc-99m, Gd-153 …) and imaging geometries (point, line, sheet source …) [5-12]. The finite intrinsic spatial resolution and non-ideal collimation cause an imprecision in the detected location and assumed origin of the transmission photons, which results in the blurred attenuation maps [13, 14]. For point source transmission system, Manglos *et. al.* [15] showed that the spatial resolution of the system is close to the intrinsic detector resolution. For extended sheet source transmission system, Cao and Tsui [16] showed that the spatial resolution is further decreased by the non-ideal source and camera collimation. For line-source [5, 13] or scanning line-source [10, 17] transmission systems, the spatial resolution could be different between the transverse and longitudinal directions, since in one direction the position of the source is well-defined or the source is well-collimated via electronic collimation and in another direction it should be treated as the extended source [18].

As in the emission imaging, finite spatial resolution of detector causes degradation of transmission reconstruction [13, 14]. To model the Poisson statistics in transmission imaging, compensation for the finite spatial resolution should be incorporated in the iterative transmission reconstruction algorithms [19, 20], which models the overall blur caused by the finite intrinsic resolution and non-ideal source and camera collimation. For an ideal system with perfect resolution, a photon is detected in a certain detector bin. For a realistic system with finite resolution, the system-blur-function (SBF) is defined to describe the probability of detecting that photon in other detector bins. This is an approximation in which the imaging system is assumed with an ideal system matrix and counts disperse into neighboring detector bins due to the finite spatial resolution.

Erdoğan and Fessler [21] proposed a monotonic transmission reconstruction algorithm called "Separable Paraboloidal Surrogates" (SPS) algorithm which models Poisson statistics in transmission imaging and can be easily penalized with piece-wise smoothness prior. The Ordered-Subset Transmission (OSTR) algorithm [22] is the ordered-subset version of SPS which accelerates efficiently the reconstruction. Our work is to incorporate compensation for the finite spatial resolution of detector into the OSTR algorithm. Similar to the derivation of the SPS and OSTR algorithms, we adopted optimization transfer principle [23, 24] which transfers the original optimization task to another easier optimization task or series of easier tasks. We derived the formulation for detector spatial resolution compensation in the frame of the SPS algorithm and adapted it to the OSTR algorithm, and finally in DISCUSSIONS we adapted it to compensation for the finite energy resolution of detector. To

make our derivation general, we made no assumptions on the form of the system-blur-function.

II. METHODS

In transmission imaging, the measurement model is

$$y_i \sim Poisson\{\bar{y}_i\} ,$$

where $i = 1,...,n_d$ denotes the detector index, the measurement means for a detector with ideal spatial resolution are

$$\bar{y}_i^0(\mathbf{x}) = b_i e^{-[\mathbf{Ax}]_i} + r_i , (1)$$

where $\mathbf{x} = [x_1 ... x_j ... x_{n_p}]^T$ is a vector describing the three-dimensional distribution of the linear attenuation coefficient, n_p is the number of voxels, $\mathbf{A} = \{a_{ij}\} \in \Re^{n_d \times n_p}$ denotes the system matrix for the transmission system, $\bar{y}_i^0$, b_i, and r_i are the ideal counts, blank scan, and average background (like scatter or crosstalk) at i^{th} detector bin, respectively. For a realistic detector with system-blur-function $G = \{g_{im}\} \in \Re^{n_d \times n_d}$, where g_{im} denotes the detection probability of $\bar{y}_i^0$ in m^{th} detector, the measurement means for this realistic detector are

$$\bar{y}_i(\mathbf{x}) = \sum_{m=1}^{n_d} g_{im} \bar{y}_m^0 = \sum_{m=1}^{n_d} g_{im}(b_m e^{-[\mathbf{Ax}]_m} + r_m)$$
$$= \sum_{m=1}^{n_d} g_{im} b_m e^{-[\mathbf{Ax}]_m} + \sum_{m=1}^{n_d} g_{im} r_m , (2)$$

where $g_{im} \neq 0$ only for rays within the same projection view, since there is no blurring from one projection view into another . If we define $b_{im} \equiv g_{im} b_m$, $R_i \equiv \sum_{m=1}^{n_d} g_{im} r_m$, we have

$$\bar{y}_i(\mathbf{x}) = \sum_{m=1}^{n_d} b_{im} e^{-[\mathbf{Ax}]_m} + R_i . (3)$$

The negative log-likelihood is

$$\psi(\mathbf{x}) = \sum_{n=1}^{n_d} \kappa(y_i, \bar{y}_i(\mathbf{x})) , (4)$$

where the *KL divergence* $\kappa(u,v) \equiv u \log \frac{u}{v} - u + v$, so the gradient

$$\frac{\partial \psi(\mathbf{x})}{\partial x_j} = \sum_{i=1}^{n_d} (1 - \frac{y_i}{\bar{y}_i(\mathbf{x})}) \frac{\partial \bar{y}_i(\mathbf{x})}{\partial x_j} = \sum_{i=1}^{n_d} [(1 - \frac{y_i}{\bar{y}_i(\mathbf{x})}) \sum_{m=1}^{n_d} b_{im} e^{-[\mathbf{Ax}]_m} (-a_{mj})]$$
$$= \sum_{m=1}^{n_d} [(-a_{mj}) b_m e^{-[\mathbf{Ax}]_m} \sum_{i=1}^{n_d} (1 - \frac{y_i}{\bar{y}_i(\mathbf{x})}) g_{im} . (5)$$

Instead minimizing $\psi(\mathbf{x})$ directly, we tried to construct the separable surrogate function of $\psi(\mathbf{x})$ [21, 22]. By minimizing or decreasing the surrogate function at each iteration, the optimization transfer principle will guarantee a monotonic decrease of $\psi(\mathbf{x})$ at each iteration and convergence to at least a local minimum [21]. From (3) and (4), we have

$$\psi(\mathbf{x}) = \sum_{i=1}^{n_d} \kappa(y_i, \sum_{m=1}^{n_d} b_{im} e^{-[Ax]_m} + R_i) . (6)$$

To simplify the notation, we define $u_{im}(\mathbf{x}) \equiv b_{im} e^{-[\mathbf{Ax}]_m} + r_{im}$, and $r_{im} \equiv R_i / n_d$, then we have

$$\psi(x) = \sum_{i=1}^{n_d} \kappa(y_i, \sum_{m=1}^{n_d} u_{im}(\mathbf{x})) = \sum_{i=1}^{n_d} \kappa(y_i, \sum_{m=1}^{n_d} (\frac{u_{im}^{(n)}}{\bar{y}_i^{-(n)}}) u_{im}(\mathbf{x}) \frac{\bar{y}_i^{-(n)}}{u_{im}^{(n)}}) , (7)$$

where $u_{im}^{(n)} \equiv u_{im}(\mathbf{x}^{(n)})$, $y_i^{(n)} \equiv y_i(\mathbf{x}^{(n)})$, $\mathbf{x}^{(n)}$ is the linear attenuation coefficient vector at the nth iteration. Since $\frac{u_{im}^{(n)}}{\bar{y}_i^{-(n)}}$ is nonnegative, and $\sum_{m=1}^{n_d} \frac{u_{im}^{(n)}}{\bar{y}_i^{-(n)}} = 1$, and since $\kappa(u,v) = \kappa_u(v)$ is convex for v , we applied De Pierro's multiplicative trick [23], and generated the following surrogate function

$$\varphi_1^{(n)}(\mathbf{x}) \equiv \sum_{i=1}^{n_d} \sum_{m=1}^{n_d} \frac{u_{im}^{(n)}}{\bar{y}_i^{-(n)}} \kappa(y_i, u_{im}(\mathbf{x}) \frac{\bar{y}_i^{-(n)}}{u_{im}^{(n)}}) \geq \psi(\mathbf{x}) . (8)$$

Using the scaling property $\alpha \kappa(u, v/\alpha) = \kappa(\alpha u, v)$, we have

$$\varphi_1^{(n)}(\mathbf{x}) = \sum_{i=1}^{n_d} \sum_{m=1}^{n_d} \kappa(\frac{u_{im}^{(n)}}{\bar{y}_i^{-(n)}} y_i, u_{im}(\mathbf{x})) = \sum_{i=1}^{n_d} \sum_{m=1}^{n_d} \kappa(y_{im}^{(n)}, u_{im}(\mathbf{x}))$$
$$= \sum_{i=1}^{n_d} \sum_{m=1}^{n_d} h([\mathbf{Ax}]_m ; y_{im}^{(n)}, b_{im}, r_{im}) , (9)$$

where $y_{im}^{(n)} \equiv \frac{u_{im}^{(n)}}{\bar{y}_i^{-(n)}} y_i$, and $h(t; y, b, r) \equiv \kappa(y, be^{-t} + r)$. The surrogate function for $h(t; y, b, r)$ [21] is

$$q(t; y, b, r, s) \equiv h(s; y, b, r) + \dot{h}(s; y, b, r)(t - s) + \tilde{c}(s; y, b, r) \frac{1}{2}(t - s)^2 , (10)$$
$$\geq h(t; y, b, r)$$

for $\forall s \in \Re$, where $\dot{h}(s; y, b, r) = \frac{\partial}{\partial t} h(t; y, b, r)$, $\tilde{c}(s; y, b, r)$ is defined in [21]. Substituting (10) into (9), we have the following inequality

$$\varphi_1^{(n)}(\mathbf{x}) \leq \sum_{i=1}^{n_d} \sum_{m=1}^{n_d} q([\mathbf{Ax}]_m; y_{im}^{(n)}, b_{im}, r_{im}, [\mathbf{Ax}^{(n)}]_m) \equiv \varphi_2^{(n)}(\mathbf{x})$$
$$= \sum_{i=1}^{n_d} \sum_{m=1}^{n_d} h([\mathbf{Ax}^{(n)}]_m; y_{im}^{(n)}, b_{im}, r_{im})$$
$$+ \sum_{i=1}^{n_d} \sum_{m=1}^{n_d} \dot{h}([\mathbf{Ax}^{(n)}]_m; y_{im}^{(n)}, b_{im}, r_{im})([\mathbf{Ax}]_m - [\mathbf{Ax}^{(n)}]_m) , (11)$$
$$+ \sum_{m=1}^{n_d} \frac{1}{2}([\mathbf{Ax}]_m - [\mathbf{Ax}^{(n)}]_m)^2 \tilde{\tilde{c}}_m^{(n)}$$

where $\tilde{\tilde{c}}_m^{(n)} \equiv \sum_{i=1}^{n_d} \tilde{c}_{im}^{(n)}$, and $\tilde{c}_{im}^{(n)} \equiv \sum_{i=1}^{n_d} \tilde{c}([\mathbf{Ax}^{(n)}]_m; y_{im}^{(n)}, b_{im}, r_{im})$.

Further we rewrite $\varphi_2^{(n)}(\mathbf{x})$ as

$$\varphi_2^{(n)}(\mathbf{x}) = \psi(\mathbf{x}^{(n)}) + (\nabla \psi(\mathbf{x}^{(n)}))^T (\mathbf{x} - \mathbf{x}^{(n)})$$
$$+ \frac{1}{2}(\mathbf{x} - \mathbf{x}^{(n)})^T \mathbf{A}^T diag\{\tilde{\tilde{c}}_m^{(n)}\} \mathbf{A}(\mathbf{x} - \mathbf{x}^{(n)}) , (12)$$

where $(\nabla \psi(\mathbf{x}^{(n)}))^T$, $(\mathbf{x} - \mathbf{x}^{(n)})^T$, and $\mathbf{A}^T$ are transposes of $\nabla \psi(\mathbf{x}^{(n)})$, $(\mathbf{x} - \mathbf{x}^{(n)})$, and $\mathbf{A}$, respectively, $diag\{\tilde{\tilde{c}}_m^{(n)}\} \equiv \{\tilde{\tilde{c}}_m^{(n)} \delta_{mj}\} \in \Re^{n_d \times n_d}$, $\delta_{mj} = 1$ for $m = j$, otherwise $\delta_{mj} = 0$. Using inequality [21] $\mathbf{B}^T diag\{w_i\} \mathbf{B} \leq diag\{\sum_{i=1}^{n_d} w_i b_{ij} b_i\}$, for any matrix $\mathbf{B} = \{b_{ij}\} \in \Re^{n_d \times n_p}$, where $b_i \equiv \sum_{j=1}^{n_p} |b_{ij}|$, we have

$$\mathbf{A}^T diag\{\widetilde{c}_m^{(n)}\}\mathbf{A} \le diag\{\sum_{m=1}^{n_d}\widetilde{c}_m^{(n)}a_{mj}a_m\} \equiv diag\{d_j^{(n)}\} \ , \quad (13)$$

where $a_m \equiv \sum_{j=1}^{n_p}|a_{mj}| = \sum_{j=1}^{n_p}a_{mj}$, and $d_j^{(n)} \equiv \sum_{m=1}^{n_d}\widetilde{c}_m^{(n)}a_{mj}a_m$. Substituting (13) into (12), we obtained a separable surrogate function

$$\begin{aligned}\varphi_3^{(n)}(\mathbf{x}) = \psi(\mathbf{x}^{(n)}) + (\nabla\psi(\mathbf{x}^{(n)}))^T(\mathbf{x} - \mathbf{x}^{(n)}) \\ + \frac{1}{2}(\mathbf{x} - \mathbf{x}^{(n)})^T diag\{d_j^{(n)}\}(\mathbf{x} - \mathbf{x}^{(n)}) \ge \varphi_2^{(n)}(\mathbf{x})\end{aligned} \ . \quad (14)$$

Minimizing $\varphi_3^{(n)}(\mathbf{x})$ and enforcing the non-negativity constraint, we obtained $(n+1)^{th}$ update as

$$x_j^{(n+1)} = [x_j^{(n)} - \frac{1}{d_j^{(n)}}\frac{\partial\psi(\mathbf{x}^{(n)})}{\partial x_j}]_+ \quad , \quad (15)$$

where operator $[a]_+ = a$ for $a > 0$, zero otherwise. From (5) we have the gradient

$$\frac{\partial\psi(\mathbf{x}^{(n)})}{\partial x_j} = \sum_{m=1}^{n_d}[(-a_{mj})b_m e^{-[\mathbf{Ax}^{(n)}]_m}\sum_{i=1}^{n_d}(1 - \frac{y_i}{\overline{y}_i(\mathbf{x}^{(n)})})g_{im}. \quad (16)$$

To calculate the gradient as in (16), one should perform one forward-blur in $\overline{y}_i(\mathbf{x}^{(n)}) = \sum_{m=1}^{n_d}g_{im}(b_m e^{-[\mathbf{Ax}^{(n)}]_m} + r_m)$ and one back-blur in $\sum_{i=1}^{n_d}(1 - \frac{y_i}{\overline{y}_i(\mathbf{x}^{(n)})})g_{im}$. Taking into account $g_{im} \ne 0$ only for rays within the same projection view, these blurring steps are performed frame-by-frame within projection/backprojection process and does not affect severely the reconstruction. By far the monotonicity still holds.

To adapt our method to the OSTR algorithm, we replaced the sum over m in (16) with the sum over subsets of the rays, and approximated $d_j^{(n)}$ with d_j which is independent of the iteration number to achieve fast implementation [22]. From (13) we have

$$\begin{aligned}d_j^{(n)} &\equiv \sum_{m=1}^{n_d}\widetilde{c}_m^{(n)}a_{mj}a_m = \sum_{m=1}^{n_d}a_{mj}a_m\sum_{i=1}^{n_d}\widetilde{c}_{im}^{(n)} \\ &= \sum_{m=1}^{n_d}a_{mj}a_m\sum_{i=1}^{n_d}\widetilde{c}([\mathbf{Ax}^{(n)}]_m; y_{im}^{(n)}, b_{im}, r_{im}) \\ &\approx \sum_{m=1}^{n_d}a_{mj}a_m\sum_{i=1}^{n_d}y_{im}^{(n)} = \sum_{m=1}^{n_d}a_{mj}a_m\sum_{i=1}^{n_d}\frac{u_{im}^{(n)}}{\overline{y}_i^{(n)}}y_i\end{aligned} \quad . \quad (17)$$

Since the blur caused by the finite detector resolution is weak, we approximated $\frac{u_{im}^{(n)}}{\overline{y}_i^{(n)}} \approx \delta_{im}$, where $\delta_{im} = 1$ if $i = m$, otherwise $\delta_{im} = 0$. Continuing on (17), we have

$$d_j^{(n)} \approx \sum_{m=1}^{n_d}a_{mj}a_m\sum_{i=1}^{n_d}y_i\delta_{im} = \sum_{m=1}^{n_d}a_{mj}a_m y_m \equiv d_j \ . \quad (18)$$

Finally we obtained the formulation of incorporating the detector resolution compensation in the OSTR algorithm

$$x_j^{(n+1)} = \left[x_j^{(n)} + \frac{M\sum_{m\in S}a_{mj}b_m e^{-[\mathbf{Ax}^{(n)}]_m}\sum_{i=1}^{n_d}(1 - \frac{y_i}{\overline{y}_i(\mathbf{x}^{(n)})})g_{im}}{d_j}\right]_+ , \quad (19)$$

where S is one of M subsets of the rays. For simplicity we omitted the usual terms for regularization [21]. Taking into account $g_{im} \ne 0$ only for rays within the same projection view, we rewrite (19) explicitly as

$$x_j^{(n+1)} = \left[x_j^{(n)} + \frac{M\sum_{m\in S}a_{mj}b_m e^{-[\mathbf{Ax}^{(n)}]_m}\sum_{i\in S}(1 - \frac{y_i}{\overline{y}_i(\mathbf{x}^{(n)})})g_{im}}{d_j}\right]_+ , \quad (20)$$

where $\overline{y}_i(\mathbf{x}^{(n)}) = \sum_{m'\in S}(b_{m'}e^{-[\mathbf{Ax}^{(n)}]_{m'}} + r_{m'})$.

III.   SIMULATIONS AND RESULTS

Our method applies to various transmission geometries. As a special case to evaluate our method, we approximately simulated the transmission acquisition of a digital rod phantom (Fig. 1) using a SPECT camera equipped with sheet source and parallel collimators. The blur on camera is attributed to two parts. One is from the finite intrinsic resolution of the camera, assumed a two dimensional (2D) Gaussian with 5 mm FWHM. The second is from the non-ideal source and camera collimation, assumed a 2D Gaussian with 12 mm FWHM when measured at the source position, which was 70 cm from the camera. The radius-of-rotation was assumed 30 cm. The rod phantom consists of three groups of uniform cylindrical rods whose radii are 2, 3, and 4 pixels, respectively. The size of detector bin is 3.17 mm, the same as the pixel size into which the rod phantom was digitized (with a 50-fold sub-sampling). We used a ray-driven cone-beam projector to generate 120-frame transmission projections through 360 degrees, modeling the source and camera collimation blur by multiplying each cone-beam ray with a weight calculated from the 2D Gaussian with 12 mm FWHM. To simulate the intrinsic blur caused by the finite intrinsic resolution, the transmission projections were further smoothed by a two-dimensional Gaussian with 5 mm FWHM. The average system-blur-function was calculated at the center of object, which was a 2D Gaussian with 7.2 mm FWHM, taking into account the contributions from collimations (5.1 mm FWHM) and intrinsic resolution (5 mm FWHM).

The resultant noise-free transmission projections were reconstructed using the OSTR algorithm with and without compensation for the finite spatial resolution. A weak regularization term with Huber's type [25] was included each case. Each case we stopped the reconstruction at the 50th iteration. The reconstructions are shown in Figure 2. From the simulation it was clear that inclusion of the detector resolution compensation greatly enhanced the resolution and accuracy of the transmission reconstruction.

IV.   DISCUSSIONS

We derived the formulation of compensation for the finite spatial resolution of detector in the transmission

reconstruction with the OSTR algorithm. Though it was derived for compensation of the finite spatial resolution, it could be adapted to compensation for the finite energy resolution of detector. If we assume that monoenergetic photons disperse into the nearby energy bins according to one-dimensional energy-response-function, there is analogy between compensation for energy resolution and compensation for spatial resolution. Following the above derivation, we could arrive at the same formulation as (20), except for interpreting that the forward-blur and back-blur in (20) are performed in the energy dimension.
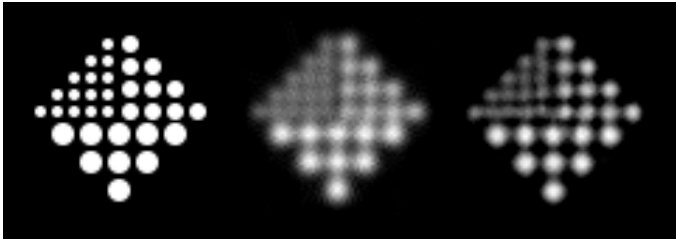
Fig. 1. (Left) The trans-axial view of original digital rod phantom. (Middle) Trans-axial view of the OSTR reconstructions from the noise-free transmission projections simulated for a parallel detector with a 12 mm collimation resolution and 5 mm intrinsic resolution, without detector resolution compensation. (Right)With detector resolution compensation for the average blurring measured at the center of the object.

V. CONCLUSION

We developed a method of incorporating the compensation for the finite spatial and energy resolution of detector in the OSTR algorithm for the transmission reconstruction in SPECT, which enhances the resolution and accuracy of the attenuation map, and therefore enhances the attenuation compensation for the emission reconstruction.

VI. REFERENCES

[1] M. A. King, B. M. W. Tsui, and T.-S. Pan, "Attenuation compensation for cardiac sigle-photon emission computed tomography imaging: Part 1. Impact of attenuation and methods of estimating attenuation maps," *J. Nucl. Card.*, vol. 2, pp. 513-524, 1995.

[2] S. J. Glick, B. C. Penney, M. A. King, and C. L. Byrne, "Noniterative compensation for the distance-dependent detector response and photon attenuation in SPECT imaging," *IEEE Trans. Med. Imag.*, vol. 13, pp. 363-374, 1994.

[3] G. L. Zeng, G. T. Gullberg, B. M. W. Tsui, and J. A. Terry, "Three-dimensional iterative reconstruction algorithm with attenuation and geometric point response correction," *IEEE Trans. Nucl. Sci.*, vol. 38, pp. 693-702, 1991.

[4] B. M. W. Tsui, H. B. Hu, D. R. Gilland, and G. T. Gullberg, "Implementation of simultaneous attenuation and detector response correction in SPECT," *IEEE Trans. Nucl. Sci.*, vol. 35, pp. 778-783, 1988.

[5] G. T. Gullberg, H. T. Morgon, G. L. Zeng, P. E. Christian, E. V. R. Di Bella, C.-H. Tung, P. J. Maniawski, Y.-L. Hsieh, and F. L. Datz, "The design and performance of a simultaneous transmission and emission tomography system," *IEEE Trans. Nucl. Sci.*, vol. 45, p. 1676, 1998.

[6] G. L. Zeng, G. T. Gullberg, and P. E. Christian, "Asymmetric Cone-Beam Transmission Tomography," *IEEE Trans Nucl Sci*, vol. 48, pp. 117-124, 2002.

[7] D. Gagnon, C. H. Tung, G. L. Zeng , and W. Hawkins, "Design and early testing of a new medium-energy transmission device for attenuation correction in SPECT and PET," *Conference Record of the 1999 IEEE Nuclear Science Symposium,* Seattle, WA, Oct, 24-30.

[8] B. Feng, M. A. King, G. L. Zeng, P. H. Pretorius, P. P. Bruyant, R. Beach, G. Boening, G. Jarkewicz, S. Cochoff, and D. Gagnon, "The estimation of attenuation maps for cardiac-SPECT using cone-beam imaging of high-energy photons through parallel-hole collimators," *IEEE Trans. Nucl. Sci.,* vol. 51, pp. 2699-2704, 2004.

[9] F. J. Beekman, C. Kamphuis, B. F. Hutton, and P. P. van Rijk, "Half-fanbeam collimators combined with scanning point sources for simultaneous emission-transmission imaging," *J. Nucl. Med.,* vol. 39, pp. 1996-2003, 1998.

[10] H. du Raan, P. D. du Toit, A. van Aswegen, M. G. Lotter, C. P. Herbst, T. N. van der Walt, and A. C. Otto, "Implementation of a Tc-99m and Ce-139 scanning line source for attenuation correction in SPECT using a dual opposing detector scintillation camera," *Med. Phys.,* vol. 27, pp. 1523-1534, 2000.

[11] D. F. Yu, J. A. Fessler, E. P. Ficaro, "Maximum-likelihood transmission image reconstruction for overlapping transmission beams," *IEEE Tr. Med. Im.*, vol. 19, pp. 1094-1105, 2000.

[12] J. E. Bowsher, M. P. Tornai, J. Peter, D. E. González Trotter, A. Krol, D. R. Gilland, and R. J. Jaszczak, "Modeling the axial extension of a transmission line source within iterative reconstruction via multiple transmission sources," *IEEE Tr. Med. Im.*, vol. 21, pp. 200-215, 2002.

[13] D. R. Gilland, R. J. Jaszczak, T. G. Turkington, and R. E. Coleman, "Comparison of transmission acquisition approaches for SPECT nonuniform attenuation compensation," *IEEE Trans. Nucl. Sci.*, vol. 45, pp. 1244-1249, 1998.

[14] M. P. Tornai, J. E. Bowsher, C. D. Stone, R. J. Jaszczak, and G. Enos, "Evaluation of transmission source collimation for SPECT attenuation compensation," in *Conf. Rec. 1999 IEEE Nuclear Science Symp. Medical Imaging Conf.,* Seattle, WA, Oct. 24-30.

[15] S. H. Manglos, D. A. Bassano, and F. D. Thomas, "Cone-beam transmission computed tomography for nonuniform attenuation compensation of SPECT images," *J. Nucl. Med.,* vol. 32, pp. 1813-1820, 1991.

[16] Z. J. Cao and B. M. W. Tsui, "Performance characteristics of transmission imaging using a uniform sheet source with parallel-hole collimation," *Med. Phys.,* vol. 19, pp. 1205-1212, 1992.

[17] P. Tan, D. L. Bailey, S. R. Meikle, S. Eberl, R. R. Fulton, and B. F. Hutton, "A scanning line source for simultaneous emission and transmission measurements in SPECT," *J. Nucl. Med.,* vol. 34, pp. 1752-1760, 1993.

[18] B. J. Kemp, F. S. Prato, and R. L. Nicholson, "The geometric modulation transfer function of a transmission imaging system that uses a SPECT scintillation camera and parallel hole collimation*," Med. Phys.*, vol. 26, pp. 733-741, 1995.

[19] J. M. Ollinger, "Maximum-likelihood reconstruction of transmission images in emission computed tomography via the EM algorithm," *IEEE Tr. Med. Im.*, vol. 21, pp. 89-101, 1994.

[20] K. Lange and R. Carson, "EM reconstruction algorithms for emission and transmission tomography," *J. Comput. Assist. Tomogr.*, vol. 8, pp. 306-316, 1984.

[21] H. Erdoğan and J. A. Fessler, "Monotonic Algorithms for Transmission Tomography", *IEEE Tr. Med. Im.*, vol. 18, pp. 801-814, 1999.

[22] H. Erdoğan and J. A. Fessler, "Ordered Subsets Algorithms for Transmission Tomography," *Phys. Med. Biol.,* vol. 44, pp. 2835-51, 1999.

[23] A. R. De Pierro, "On the relation between the ISRA and the EM algorithm for positron emission tomography," *IEEE Tr. Med. Im.*, vol. 12, pp. 328-333, 1993.

[24] K. Lange, *Numerical analysis for statisticians*, Springer-Verlag, New York, 1999.

[25] P. J. Huber, *Robust Statistics*, Wiley, New York, 1981.